

## Highly Emissive Phosphorescence Nanoparticles Sensitized by a TADF Polymer for Time-resolved Luminescence Imaging

Li Xu<sup>\*a</sup>, Jin Wang<sup>a</sup>, Qingqing Luo<sup>a</sup>, Guangcai Chen<sup>a</sup>, Fan Ni<sup>b</sup>, Zece Zhu<sup>\*c</sup>, Qiang Zhao<sup>\*d</sup>, Guojun Zhang<sup>a</sup> and Chuluo Yang<sup>\*b</sup>

<sup>a</sup> Department of Pharmacy, Hubei University of Chinese Medicine, Wuhan 430065, P. R. China. E-mail: [xul1819009@126.com](mailto:xul1819009@126.com)

<sup>b</sup> College of Materials Science and Engineering, Shenzhen University, Shenzhen 518060, P. R. China. Email: [clyang@szu.edu.cn](mailto:clyang@szu.edu.cn)

<sup>c</sup> Wuhan National Laboratory for Optoelectronics & School of Optical and Electronic Information, Huazhong University of Science and Technology, Wuhan 430074, P. R. China. E-mail: [zece@hust.edu.cn](mailto:zece@hust.edu.cn)

<sup>d</sup> Key Laboratory for Organic Electronics and Information Displays & Jiangsu Key Laboratory for Biosensors, Institute of Advanced Materials (IAM), Nanjing University of Posts and Telecommunications, Nanjing, 210023, China. E-mail: [iamqzhao@njupt.edu.cn](mailto:iamqzhao@njupt.edu.cn)

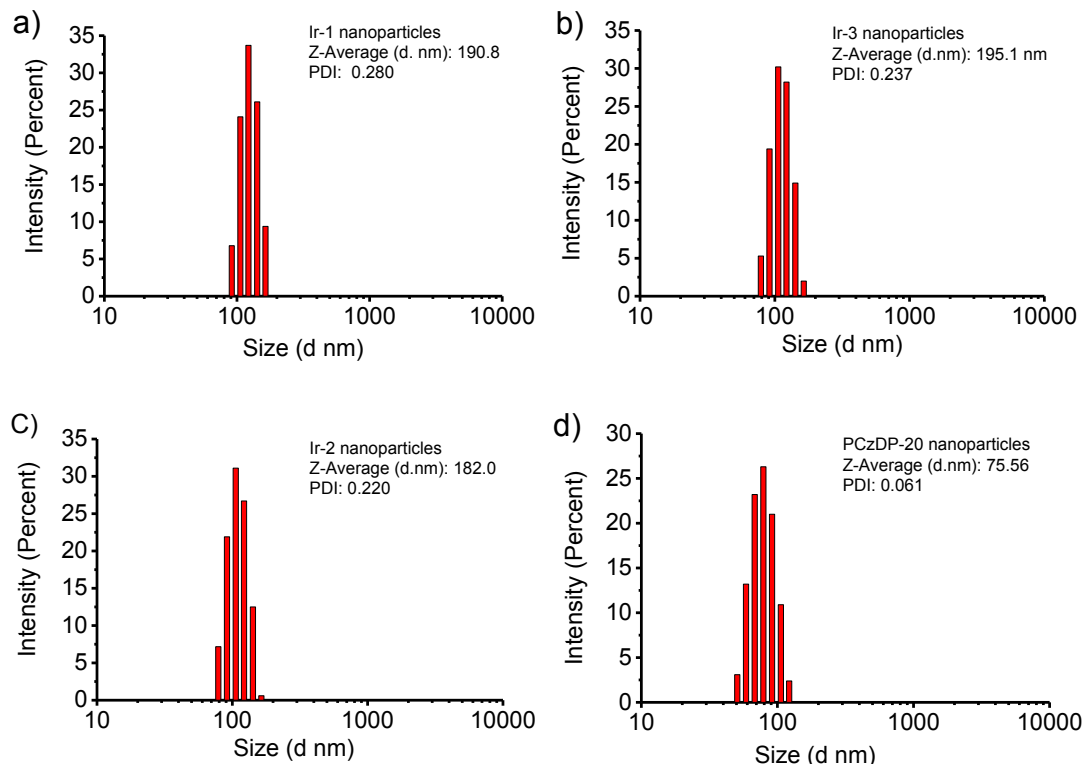


Figure S1. DLS histograms of a) Ir-1, b) Ir-3, c) Ir-2, and d) PCzDP-20 nanoparticles.  $[Ir-1] = [Ir-2] = [Ir-3] = 5 \mu\text{g mL}^{-1}$ .

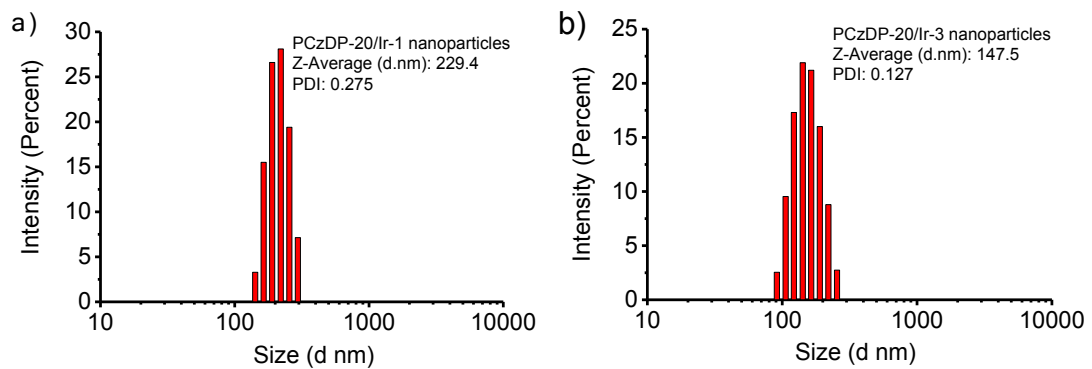


Figure S2. DLS histograms of a) PCzDP-20/Ir-1 and b) PCzDP-20/Ir-3 nanoparticles.  $[PCzDP-2] = 200 \mu\text{g mL}^{-1}$ ,  $[Ir-1] = [Ir-3] = 5 \mu\text{g mL}^{-1}$ .

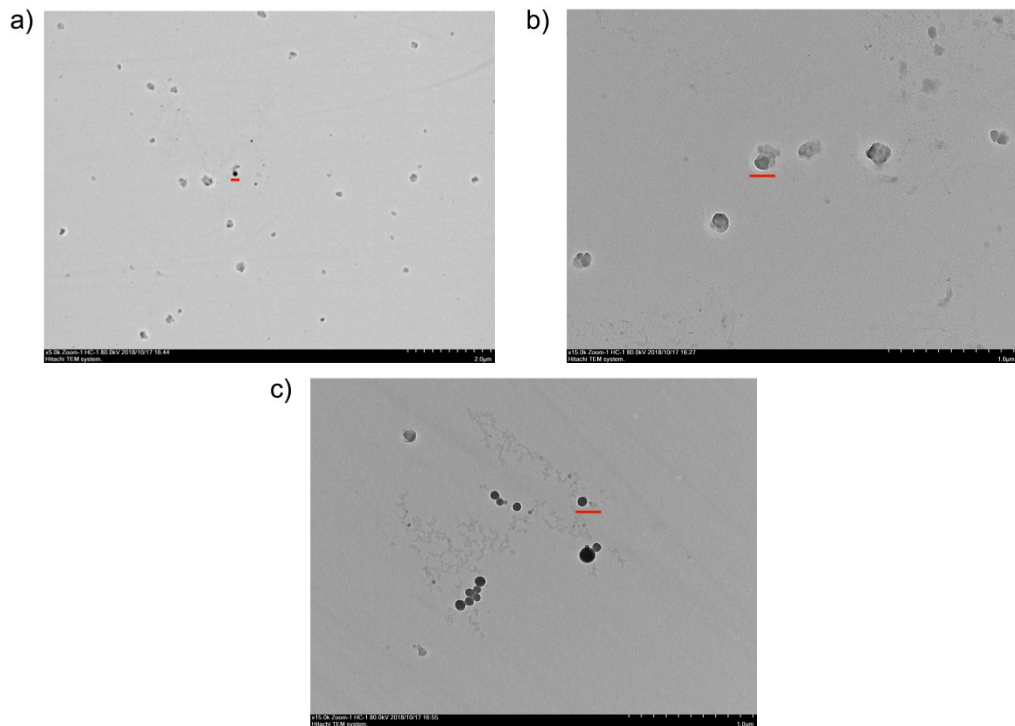


Figure S3. TEM images of 2.5% doped a) PCzDP-20/Ir-1, b) PCzDP-20/Ir-2 and c) PCzDP-20/Ir-3 nanoparticles. Scale bar = 200 nm for all images.

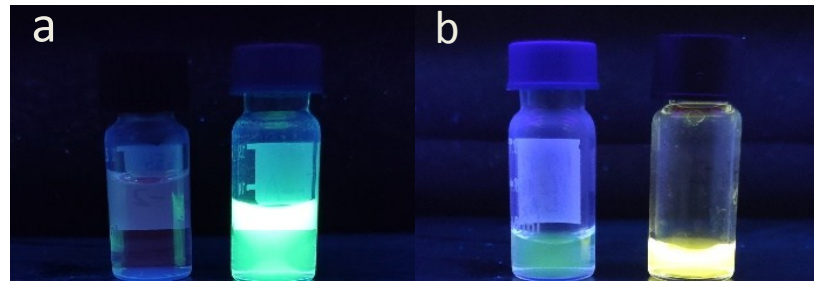


Figure S4. Fluorescence images of a) undoped Ir-2 nanoparticles ( $5 \mu\text{g mL}^{-1}$ ) (left) and PCzDP-20 nanoparticles ( $200 \mu\text{g mL}^{-1}$ ) (right). b) The mixed solution of Ir-2 nanoparticles and PCzDP-20 nanoparticles by 1:1 volume (left), and the mixed solution of water and doped PCzDP-20/Ir-2 nanoparticles by 1:1 volume (right).

As Figure S1 showed, undoped Ir-2 nanoparticles could be prepared by  $5 \mu\text{g mL}^{-1}$  Ir-2 complex, with a larger Z-average diameter than that of 2.5 % doped PCzDP-20/Ir-2 nanoparticles. We had tried to prepare the undoped nanoparticles of  $30 \mu\text{g mL}^{-1}$  Ir-2 complex, but the formed dispersion medium could hardly pass through a  $0.45 \mu\text{m}$  filter. We speculated that the rigid Ir complex molecules trend to self-aggregated when dropped into water with a high concentration, thus the formed dispersion medium has a larger size that may exceed nanoscale and it was impossible to increase the luminescence intensity of undoped Ir(III) nanoparticles by increasing the concentration of Ir(III) complex molecules encapsulated in nanocarriers. Meanwhile, the result of Figure 1d confirmed that the polymer PCzDP-20 was more dispersed than Ir(III) complexes in nanoparticles, which had a smaller size. We thought that it is because of the particular characteristics of PCzDP-20, homogenous doping of Ir(III) complexes with PCzDP-20 in nanocarriers could be realized. And only by homogenous Ir(III) complexes doping with PCzDP-20 could realize an efficient EnT. As Figure S4 showed, when the undoped Ir-2 nanoparticles ( $5 \mu\text{g mL}^{-1}$ ) and PCzDP-20 nanoparticles ( $200 \mu\text{g mL}^{-1}$ ) were mixed together by 1:1 volume, it still emitted green emission since there was no energy transfer from PCzDP-20 to Ir-2 complex. Only homogenous doped PCzDP-20/Ir-2 nanoparticles solution (also mixed with water by 1:1 volume) could emit a strong orange emission from Ir-2 complex

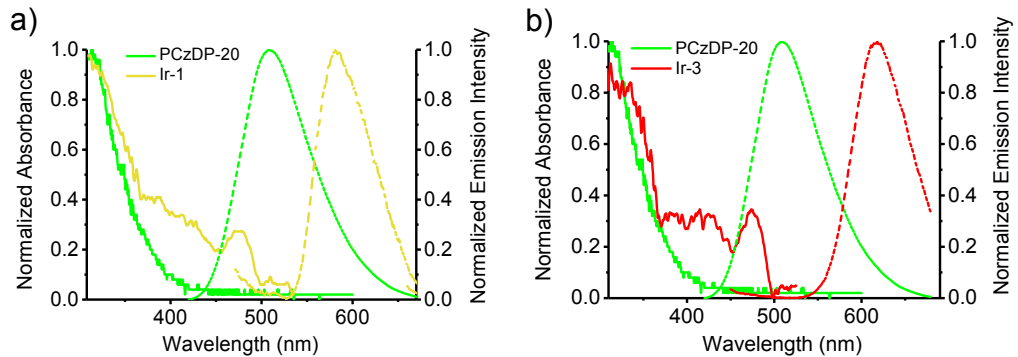


Figure S5. Absorption (solid line) and emission spectra (dotted line) of PCzDP-20 nanoparticles (green line) and a) Ir-1 nanoparticles (yellow line) and b) Ir-3 nanoparticles (red line).  $\lambda_{\text{ex}} = 355 \text{ nm}$ .

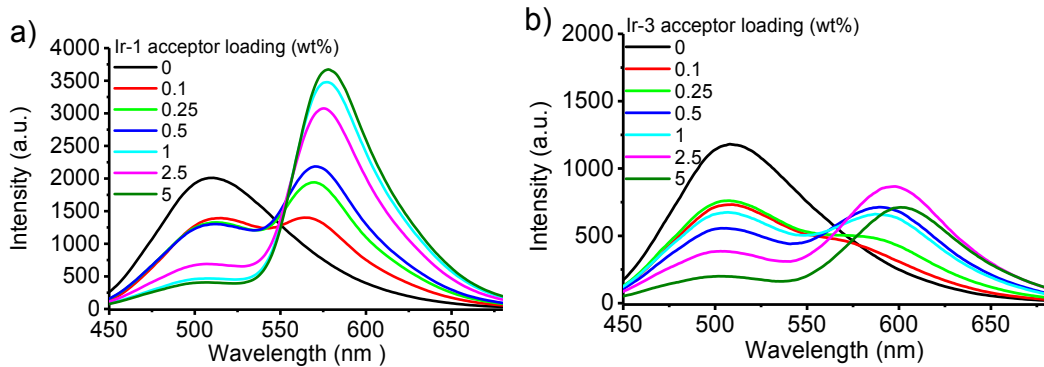


Figure S6. Emission spectra of nanoparticles doped with different amounts of a) Ir-1 acceptor and b) Ir-3 acceptor while keeping the same amount of the TADF polymer donor ( $200 \mu\text{g mL}^{-1}$ ).

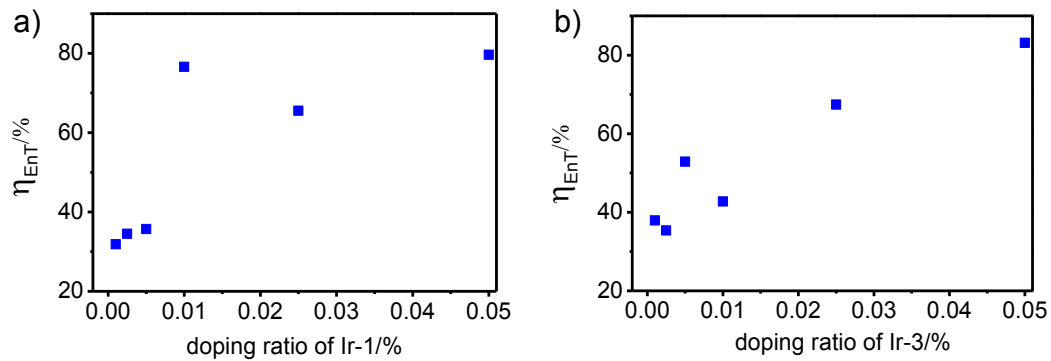


Figure S7. The energy transfer efficiency of donor emission at 507 nm as a function of the doping ratio of a) Ir-1 (left) and b) Ir-3 (right).

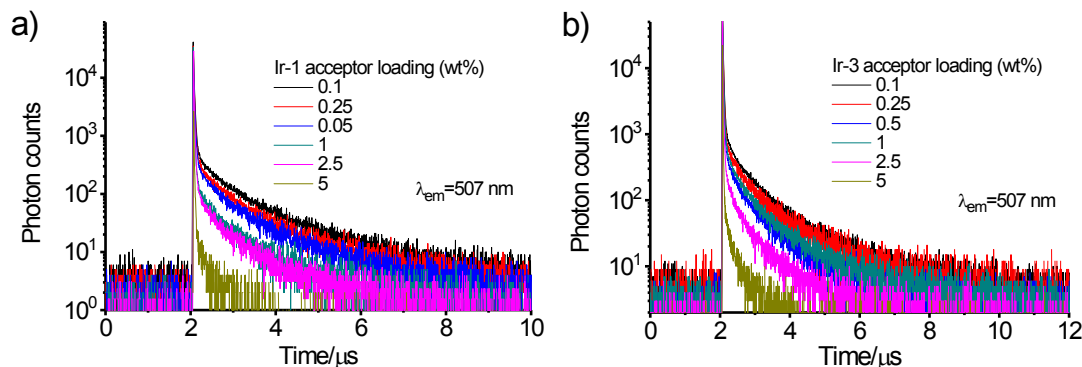


Figure S8. The luminescence decay of the PCzDP-20 doped with different amounts of a) Ir-1 and b) Ir-3 acceptor.  $[\text{PCzDP-20}] = 200 \mu\text{g mL}^{-1}$ .

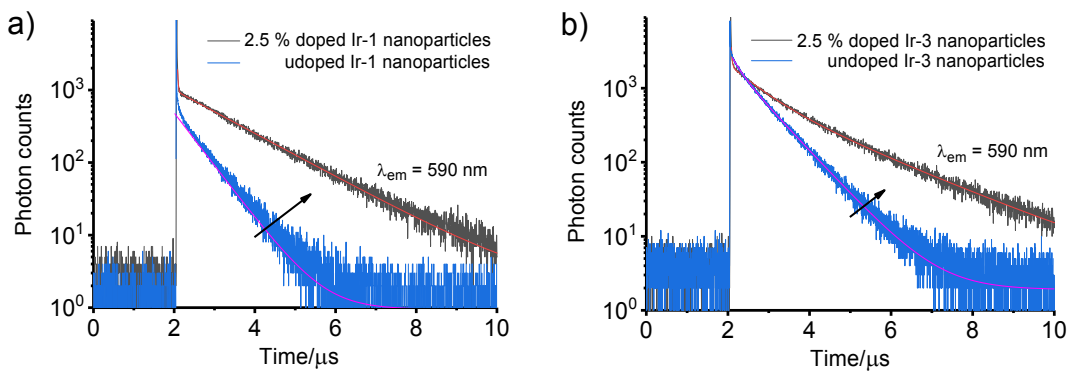


Figure S9. The luminescence decay curves of the a) Ir-1 and b) Ir-3 nanoparticles: 2.5 % doped vs undoped.  $[Ir-1] = [Ir-3] = 5 \mu\text{g mL}^{-1}$ .

Table S1. The fitting details of the luminescence decay curves of the Ir complex nanoparticles.

nanoparticles		$\tau$ (weight)	$\chi^2$
Ir-1	undoped	600 ns(100%)	0.994
	2.5% doped	15 ns (1%) 1500 ns (99%)	1.091
Ir-2	undoped	610 ns(100%)	1.533
	2.5% doped	600 ns (25%) 1300 ns (75%)	0.981
Ir-3	undoped	220 ns (11%) 740 ns (89%)	1.077
	2.5% doped	19 ns (2%)	1.1
		690 ns (32%)	
		1900 ns (66%)	

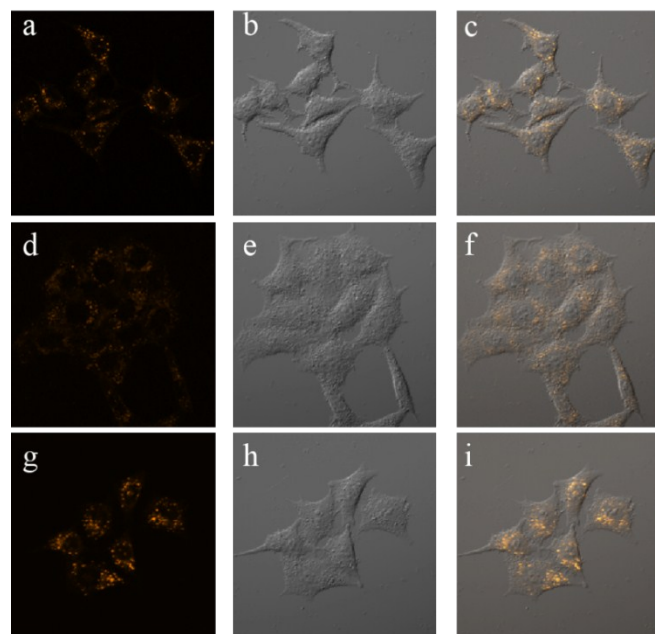


Figure S10. CLSM images of HeLa cells after incubation with Ir-1 @K.L (a-c), Ir-2@K.L (d-f), and Ir-3@K.L (g-i). Left, darkfield; Middle, bright field; Right, merging of left and middle.

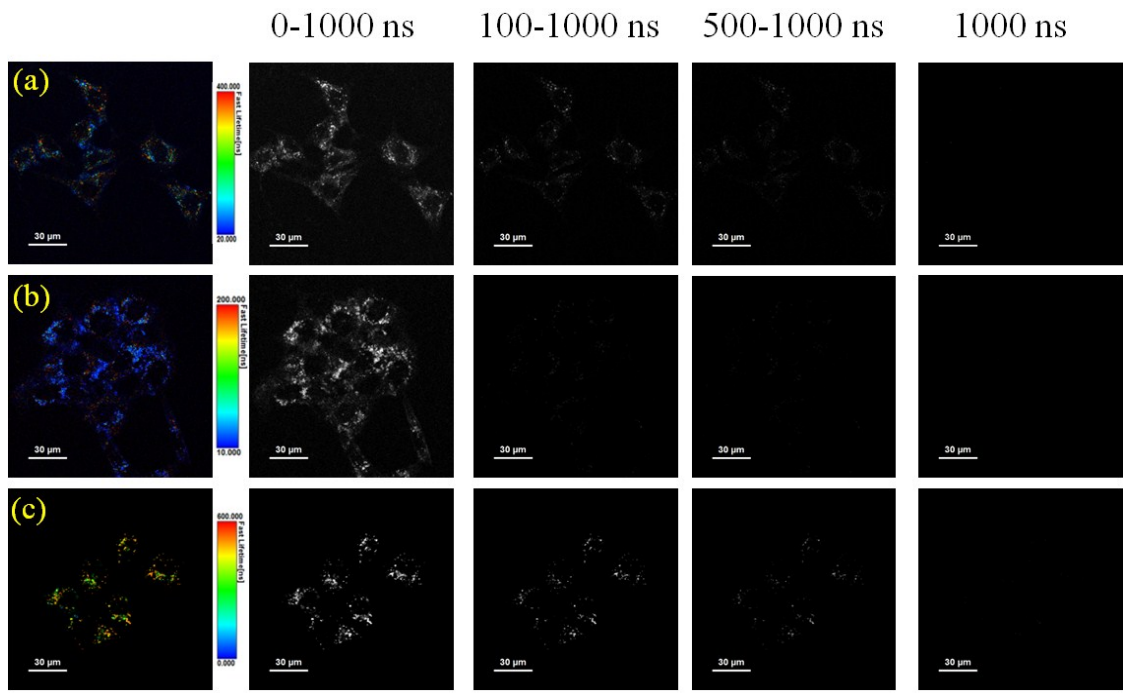


Figure S11. Luminescence lifetime (colorful) and Time-gated luminescence (black and white) images of (a) Ir-10@K.L, (b) Ir-2@K.L, and (c) Ir-3@K.L in HeLa cell.